A knowledge-driven Multi-Criteria Decision Making-Analytical Hierarchy Process based Geospatial Modeling for the Delineation of Fluoride Contamination Zones in Groundwater, Jamui District, Indo-Gangetic Alluvial Plains, India

Suresh Kumar
Central Ground Water Board
Sudhakar Singha
IIT (ISM): Indian Institute of Technology
Rambabu Singh
CMPDIL,Bilaspur
Venkatesh Satya Akella (akellasatyavenkatesh@gmail.com)
Indian School of Mines: Indian Institute of Technology https://orcid.org/0000-0002-3342-4374
Utpal Gogoi
Central Ground Water Board,Faridabad

Research Article

Keywords: Fluoride contamination, MCDM-AHP, Geospatial technology, Jamui, Indo-Gangetic Alluvial Plains

Posted Date: February 22nd, 2021

DOI: https://doi.org/10.21203/rs.3.rs-175060/v1

A knowledge-driven Multi-Criteria Decision Making- Analytical Hierarchy Process based geospatial modeling for the delineation of fluoride contamination zones in groundwater, Jamui district, Indo-Gangetic alluvial plains, India

Suresh Kumar[1&4], Sudhakar Singha[2], Rambabu Singh[3], A. S. Venkatesh[4*]

[1]Central Ground Water Board, Patna-800001, India.

[2]Department of Civil Engineering, Indian Institute of Technology (Indian School of Mines), Dhanbad-826004, Jharkhand, India.

[3]Central Mine Planning and Design Institute Limited, Bilaspur-495006, India

[4]Department of Applied Geology, Indian Institute of Technology (Indian School of Mines), Dhanbad-826004, India.

*(*Corresponding author:asvenkatesh@iitism.ac.in)*

Abstract

This study presents a framework to delineate the potential fluoride contamination zones within the groundwater of the study area by employing GIS coupled with Multi-Criteria Decision Making-Analytical Hierarchy Process approach (MCDM-AHP). In this context, various groundwater contamination controlling hydrogeo-meteorological factors thematic layers were prepared in the GIS environment and assigned with an appropriate rating and weights. All the selected influencing factors were overlaid using a weighted overlaid index approach after normalizing the weights and ratings of the respective layers using the AHP technique and then computed the fluoride contamination zones (FCZs). The obtained results indicate that 61.50% (1101.82 km^2) of the total study area was delineated as a relatively safe zone (F< 1.5 mg/L) and the remaining 38.50% (689.18 km^2) was demarcated under the unsafe zone (F>1.5 mg/L). The proposed FCZs model corroborates a significant agreement of 85% with the 61 observed locations and thus testify to the model reliability.

Keywords: Fluoride contamination, MCDM-AHP, Geospatial technology, Jamui, Indo-Gangetic Alluvial Plains.

1.0 Introduction

Fluoride is one of the essential and helpful elements for human health as it is associated with bone mineralization and dental enamel formation (Rahman et al., 2020; Gonçalveset al., 2020; Mondal et al., 2009). Moreover, some health issues are common, especially in children, such as deficiency in bone mineralization, dental enamel formation, dental caries, when the amount of fluoride consumed daily is less than 0.5 mg/L (Kumar et al., 2019). At the same time, the consumption of drinking water with a fluoride concentration of more than 1.5 mg/L leads to fluorosis, which is common in both adults and children (Kumar et al., 2019). Children and the younger populations in the fluoride endemic areas are highly affected by mottled enamel (Yuan et al., 2017). Consumption of fluoride enriched groundwater develops symptoms of skeletal fluorosis such as pain related to bones and joints in elderly people (Sawangjang et al., 2019). It has been observed that these symptoms in a long run turn into permanent disability (Liu et al., 2015).

The incidence of fluorosis and its severity is due to the presence of fluoride content in water and soil. Prolonged consumption of fluoride enriched groundwater is a crucial contributor responsible for the waterborne fluorosis in human beings (Singh et al., 2017a and b, Su et al., 2019). The chemical composition of hinterland geology or lithological unit is closely related to the higher groundwater fluoride concentration (Singha et al., 2019a; Singh et al., 2018). Many scholars in their studies have highlighted that higher fluoride levels in the groundwater of granitic and metamorphic rock terrains were ascribed to the release of fluoride ion from the host rocks (Shanker et al., 2003; Thapa et al., 2017; Su et al., 2019; Narsimha et al., 2019).

Geological materials consisting of fluoride-rich minerals such as fluorite, apatite, wohlerite, tourmaline, herderite, sphene, hornblende series minerals, muscovite, actinolite and fluor-apatite

52 can trigger fluoride enrichment in aquifer solution through prolonged rock-water interaction
53 (Todd and Mays, 2005; Rao., 2009, Adimalla and Venkatayogi, 2017). Several clay minerals,
54 namely smectite, illite and chlorite also contribute significantly to fluoride concentration in
55 solution (Tossou et al., 2017). In recent times, several researchers have opinioned that climate,
56 evaporation, adsorption-desorption, ion exchange, ion competition, alkaline environmental
57 conditions, lithology, and geomorphology of the area are the significant factors that can produce
58 fluoride enriched groundwater (Mondal et al., 2009; Luo et al., 2018; Vithanage et al., 2014).
59 The higher the surface drainage density more is the surface runoff of rainfall and scanty is the
60 infiltration to groundwater storage.
61 Fluoride contamination commonly increases when lesser infiltration of rainwater occurs (Thapa
62 et al., 2017). A flat ground surface leads to higher infiltration due to its less drainage density,
63 which may result in higher leaching of fluoride in the aquifer. Besides this, the existence of
64 fracture density in rocks is predominantly responsible for the higher propagation of fluoride
65 values in groundwater (Kim and Jeong, 2005). Moreover, certain anthropogenic activities viz.,
66 domestic sewage, excessive utilization of phosphate fertilizers and pesticides in the crop fields
67 and long-time irrigation practices are also accountable for higher fluoride levels in groundwater
68 storage through leaching (Dartan et al., 2017; Srivastava and Ramanathan, 2018). The presence
69 of excess fluoride content in the subsurface water resources has now drawn global attention as
70 one of the most detrimental menaces to human health and geo-environmental problems in India
71 and other parts of the world (Ando et al., 2001; Pillai and Stanley., 2002; Madhnure et al., 2007).
72 The present study area comprises thick granitic litho-units and initially, the elevated fluoride
73 levels in groundwater were reported in some locations of the study area by the Central Ground
74 Water Board (CGWB, 2013) in which granitic activity is prevalent. Later on, Kumar et al., (2017

and 2019) studied contamination of groundwater with respect to fluoride and its dynamic effects were assessed with the aid of hydro-geochemical signatures, chemometric methods and medical geological aspects. Notwithstanding, to the best of the knowledge of the authors, none of the studies have been reported on exploring and verifying the geospatial modeling for identification of fluoride contamination zones in the research area, where the study area is particularly important as it is characterized by both crystalline and alluvial aquifer units. Hence, in the current investigation, a knowledge driven Multi-Criteria Decision Making- Analytical Hierarchy Process (MCDM – AHP) approach coupled with the GIS environment has been exercised for delineating the spatial distribution of groundwater fluoride contamination regions in parts of Jamui district, Bihar, India. The main objectives of the study comprise of mapping fluoride affected hazardous zones by considering various geological features and assigning their optimized MCDM - AHP based weight/ratings for the computation of FCZ indices. Finally, the verification of the FCZ map was carried out with measured fluoride concentrations to evaluate the proposed model performance through which the prognostication of fluoride contamination zones can be planned.

2.0 Study area

The proposed study area is a part of Jamui district in the state of Bihar, India and lies between North latitude $24^0$40' to $25^0$10' and East longitude $85^0$50' to $86^0$35' with a total extent of 1791 km^2. The geology of the study area is composed of rocky upland, pediplain and alluvial plains. Alluvial plains in the study area were formed by continental Quaternary deposits and is a part of the Jamui Formation and is generally termed as “older alluvium” in Indian geology. The major rock types which cover the region are quartzite, quartz-mica schist, biotite-muscovite schist, granites, composite gneisses, pegmatite, amphibolite and quartz veins. The most potential

aquifers are common in the alluvial formation. The thickness of the alluvium gradually increases towards the north and finally merges with the Gangetic alluvium, south of the River Ganga. The total thickness of the alluvium ranges from 90 m in the northern part and is finally reduces to less than 12 m in the southern part. Some other landforms like, escarpment, inselbergs and valley fills are also present in the area. Humid climate dominates the area and is the driving factor responsible for the weathering of the overlying mantle. Elevated fluoride concentration in the groundwater of the study area might have been generated due to weathering of this fluoride bearing material from granite, granite-gneiss, amphibolites and mica-schists and deposition of same over the parent rock as a weathered mantle. A tropical southwestern monsoon climate governs the area with an average annual precipitation of 1042 mm. Infiltration from monsoon rainfall contributes to the major part of the recharge of aquifers.

3.0 Materials and methods

High density polyethylene bottles (HDPE) were used for the collection of water samples for fluoride analysis. Sample bottles were cleaned several times using distilled water prior to sampling. A total of 61 groundwater samples were collected in the month of May 2014 for the estimation of fluoride. The samples were analyzed for fluoride concentration using Systronic make UV-VIS spectrophotometer (2202) within two weeks after the collection of samples. The standard procedure provided by the American Public Health Association (APHA 2012) was strictly adhered during analysis.

3.1 Development of thematic layers

In order to delineate fluoride contaminated zones, a total of 10 separate thematic layers were prepared for the investigation using conventional chemical data, remote sensing (RS) and Arc

GIS 10.3. The thematic layers include aquifer (A), geomorphology (G), soil texture (S), slope/topography (T), elevation (E), drainage density (D) and distribution of rainfall (R), depth to water table (D), land use land cover (LULC) and lineament density (L). Details of the thematic layers are given in Table 1. The methodology followed is shown in Fig. 1. Geomorphological details of the region were prepared with the help of the groundwater information booklet Jamui district, Bihar, India (CGWB, 2007). Digital elevation model (SRTM, USGS) of 30 m resolution was applied to prepare the slope and elevation map of the study region. Pre-monsoon water table depth for 31 locations was measured for the entire study area in the year 2014. The lineament and land use pattern data were collected form the National Remote Sensing Centre (NRSC), Hyderabad. The study area soil map was prepared from data obtained from the National Bureau of Soil Survey and Land Use Planning (NBSSLUP). Rainfall data for 2013 to 2017 was compiled from Indian Meteorological Department (IMD) and the geological map used to be after the Geological Survey of India (1987).

"Figure 1 is about here"

3.2 Weight assignment and weight normalization factors using AHP

The Analytical Hierarchical Process (AHP), is a very effective approach for handling the complexity of real world decision-making problems, developed by Saaty (1980). A knowledge driven AHP-based multi-criteria decision analysis (MCDM) is a very much popular parameter weight prioritization approach in the prognostication of contaminants. AHP is an effective tool, which reduces the complexity associated with decision making problems into a series of pair-wise comparisons and then synthesizes the outcome of the final results (Arulbalaji et al., 2019). In addition, the AHP-based MCDM approach is also a suitable evaluation technique to evaluate the consistency of final output; accordingly, it reduces the conflict involved in the decision-

making process. Based on the above facts, in the current research work, a combined approach of AHP and GIS technique is used to delineate the fluoride contaminated zones of the area under study. The chosen ten thematic layers were supposed to be accountable for enhanced fluoride concentration in the study region. Hence, the influencing factors were weighted according to their contribution to groundwater contamination, especially with respect to fluoride, field study and keeping in mind review of past studies. A layer with a higher weight illustrates a parameter with a higher contribution towards groundwater contamination and vice versa. According to Saaty's scales (1980) of relative importance value, assigned weights for selected factors are as follows: similar importance (scale-1), moderate importance of one over another (scale-3), strong importance (scale-5), very strong importance (scale-7), extreme importance (scale-9), intermediate values between the two adjacent judgments (scale-2, 4, 6, 8), reciprocal for inverse comparison (scale-reciprocals of the above nonzero numbers). After the weight assigned to the respective factors, the relative comparison of all the factors with each other was structured to form a pair-wise comparison matrix (Table 2).

"Table 2 is about here"

Pair-wise comparison matrix (Table 2) constructed for the thematic layers is in following accordance:

$$M = \begin{bmatrix} A_{11} & A_{12}.. & A_{1n} \\ A_{21} & A_{22}.. & A_{2n} \\ : & : & : \\ A_{f1} & A_{f2}.. & A_{fn} \end{bmatrix} \quad (1)$$

Computed pair wise comparison matrix (M = [A_{fn}]) is demonstrated in Table 2 and has been exhibited by applying equation:

$$A_{fn}'' = \frac{A_{fn}}{\sum_{f=1}^{x} A_{fn}} \quad (2)$$

Where, n = 1, 2, 3, 4, 5,…….x, A_{fn} represents the element of f row besides n column of matrix.

(b) Computation of normalized weight (w_x)

The normalized weight (w_x) was calculated utilizing Eq. 3.

$$w_x = \frac{\sum_{n=1}^{x} A_{fn}''}{x} \quad (3)$$

Where, f = 1, 2, 3, 4,5,…...x

(c) Examination of uncertainty in judgment

Then to examine the uncertainty, Satty (2004) proposed the principal eigenvalue and consistency index and to examine the uniformity of judgment matrix, the consistency ratio.

Hence, for computing the consistency ratio (CR), the procedure adopted is as follows: (1) first of all, Principal Eigenvalue (λ) was figured out by Eigenvector technique and (2) secondly, Consistency Index (CI) was computed using the Eq. 4

$$CI = \frac{\lambda_{\max} - n}{n-1} \quad (4)$$

In the above mentioned equation, n represents no. of thematic layers (n = 10 in this case) whereas λ_{max} represents the maximum eigenvalue of the pair-wise comparison matrix.

Ultimately, Consistency ratio (CR) was derived by using Eq. 5.

$$CR = \frac{CI}{RCI} \quad (5)$$

Where *CI* represents the consistency index and *RCI* denotes the random consistency index, respectively. *RCI* values are considered from Saaty's (1980), 1-9 point scale for the selected

number of parameters. Saaty's ratio index (RCI) for corresponding numbers of parameters (n) is as follows: n-1 (RCI-0), n-2 (RCI-0), n-3 (RCI-0.52), n-4 (RCI-0.89), n-5 (RCI-1.11), n-6 (RCI-1.25), n-7 (RCI-1.35), n-8 (RCI-1.10), n-9 (RCI-1.45) and n-1 (RCI-1.49). Satty (1980) advocated that CR value less than 10%, defends the consistency in the pair-wise comparison. In this study, the CR value is 5.5% and thus withstands the consistency.

The normalized computed weights for all the thematic layers were finalized for further analysis. Thereafter, the subclasses of thematic layers were re-classified in the GIS platform. The ratings of subclasses of each thematic layer were allocated on a gradation of 1 to 9, according to their relative significance with respect to the contribution to the groundwater fluoride contamination.

3.3 Weighted overlay index-based approach (WOIA)

The WOIA method is utilized by a good number of researchers globally in different regions in varying hydro-geologic settings (Elewa and Qaddah., 2011; Ghazavi and Ebrahimi., 2015; Al-Abadi et al., 2017; Singha et al., 2017; Thapa et al., 2018). The ratings and weights of all the ten layers were multiplied and summed up together to demarcate fluoride contaminated zones (FCZ). FCZ for the study area has been computed by using the following equation:

$$FCZ = \sum_{1}^{n} (P_r Q_w) \qquad (6)$$

Where P and Q denote the parameters and subscript r and w are the respective ratings designated to parameter subclasses and weights to each parameter class. Hence, this is the most well-known, simple and flexible method for integrating all the thematic layers in the GIS environment. Accordingly, the final fluoride contamination zone map was classified into two categories, namely, safe and unsafe zone.

4.0 Results and discussion

4.1 Role of Hydrogeo-meteorological factors and groundwater quality

Dynamic groundwater resource of the phreatic aquifer in the study area gets replenished each year, mainly by diffuse rain fed recharge apart from that managed recharge consisting of planned and unplanned recharge through various artificial recharge structures and seepage from water bodies and irrigation fields. Water that recharges the groundwater, gets altered during its course of infiltration and precipitation thereby acquire mixed quality depending on the source and passing media (i.e. Hydrogeo-meteorological parameters). Therefore, groundwater quality and its occurrence is dependent upon various hydrogeo-meteorological factors viz., aquifer media, geomorphology, soil texture, slope, elevation, drainage density, rainfall distribution, depth to the water table, land use land cover and lineament density. On the basis of each parameter characteristics and significance in terms of potential groundwater contamination with respect to fluoride, relative rating and weights have been assigned and fluoride contaminated zones (FCZ) were demarcated after building of each thematic layer as mentioned in the following section.

Aquifer media imparts a vital role in absorption, storage, the transmission of water and the residence time of groundwater. The coarser the aquifer material, the lesser is the residence time and lesser the chances of groundwater contamination and vice versa. Based on the aquifer characteristics (media), the study area was categorized into four classes, viz., alluvial, biotite-muscovite-chloride schist, granite gneiss, quartzite, quartz schist and phyllite extending over an area of around 113 km^2, 818 km^2, 506 km^2 and 353 km^2 respectively. The aquifer map of the study region is shown in Fig. 2a.

Geomorphologic patterns are generally known as the surface indicators revealing the conditions for groundwater occurrence of a region (Preeza et al., 2011). Moreover, it also reflects the

underlying geological formation that is responsible for groundwater occurrence, storage, transmission and its residence time. Hence, the geomorphology of the study area plays an important role in groundwater studies (Machiwal et al., 2011; Singha et al., 2019b). In the study area, Quaternary alluvial plains occupy an area of about 463 km^2, denudational hills and piedmont covers an area of about 730 km^2 and pediplain covers an area of about 598 km^2 respectively. The geomorphological pattern of the study area is shown in Fig. 2b.

Soil texture is one of the influencing factors considered for any groundwater-related studies as it exhibits the infiltration rate of the soil media through which water flows and reaches the aquifer. The coarser the soil media, the lesser will be the holding capacity and more will be the chances of contaminants to reach the aquifer and vice versa. In the study area, coarse loamy soil extends over an area of about 458 km^2 approximately, whereas fine loamy soil extends over an area of about 1333 km^2. Coarse loamy soil has been assigned higher weightage due to its high infiltration rate. The soil texture map of the study area is shown in Fig. 2c.

The slope is another important factor in groundwater studies, that greatly influences the recharge of groundwater, i.e., gentle to flat slopes will contribute to less runoff, thereby increases the infiltration rate and groundwater contamination. On the contrary, segments of the study area, with higher slope (steep slope) results in a higher runoff, lower infiltration rate and consequently reduces the chances of groundwater contamination. According to the slope, the study area was categorized into five classes such as 0-3%, 3-6%, 6-9%, 9-12% and more than 12% encompassing over an area of approximately, 654 km^2, 626 km^2, 210 km^2, 65 km^2 and 236.99 km^2 respectively. The slope map of the study area is shown in Fig. 2d.

"Figure 2 is about here"

Elevation and slope of a region signify the storage of groundwater, i.e., a lower slope tends to higher groundwater storage in comparison to the areas with steeper slope (Thapa et al., 2017). In

253 the study area, around 1415 km^2 area falls in an elevation varying from 42-167 m, 297 km^2 falls
254 in between 167-292m, 70 km^2 falls within 292 to 417 m and 9 km^2 area falls in between 417-542
255 m respectively. The elevation map of the study area is shown in Fig. 2e.
256 Drainage density is known as the proximity of the spacing of the flow channels. The drainage
257 density is inversely correlated to the permeability factor. Drainage density is inversely related to
258 the permeability of aquifers (Arulbalaji et al., 2019). The higher drainage density of an area
259 indicates the presence of a less permeable lithological unit resulting in more runoff within the
260 region (Rashid et al., 2012). Hence, higher drainage density indicates low recharge and lower
261 chances of subsurface water contamination and vice versa (Bagyaraj et al., 2013). In the study
262 area, drainage density was classified into five categories such as 0-3 km/km^2 encompassing over
263 an area of around 1264 km^2, 3-6 km/km^2 extending over an area of about 369 km^2, 6-9 km/km^2
264 with 104 km^2, 9-12 km/km^2 with 45 km^2 and more than 12 km/km^2 accounts for 9 km^2
265 approximately in the study area respectively. The drainage density map of the study region in the
266 Jamui district is shown in Fig. 2f.
267 Intensity, duration, and distribution of rainfall in a region also impart a vital role in respect to
268 infiltration and contamination rate. Higher intensity and shorter duration infer the higher rate of
269 runoff and lower infiltration, hence lower chances of groundwater contamination and conversely
270 (Ibrahim-Bathis and Ahmed, 2016). The study area experiences an annual rainfall varying from
271 718 mm/year to 1071 mm/ year and was classified accordingly into three subclasses such as 718-
272 835 mm (around 117 $km^2$of total area), 835-952 mm (1225 km^2) and more than 952 mm (449
273 km^2) respectively. The rainfall distribution map of the study area is shown in Fig. 2g.
274 Depth to the water table is one of the most significant parameters amongst other selected
275 parameters as it depicts the thickness (band) of material through which contaminant travels from

276 the surface to the groundwater table before reaching an aquifer. The deeper the water table depth,
277 the lesser the possibilities of contaminants to reach within subsurface water (Senthilkumar et al.,
278 2014). Pre-monsoon water table depth has been considered for the study and was classified into
279 four categories, i.e., 0-3 m, 3-6 m, 6-9 m, more than 9 m which encompasses over an area of
280 around 5 km^2, 1138 km^2, 634 km^2, and 15 km^2respectively. The range of depth to water table
281 varies in the study area from 1.93 m to 12.06 m. The depth to water table map is shown in Fig.
282 2h.
283 Land Use Land Cover (LULC) is considered as one of the important parameters as it is
284 intimately associated with the groundwater quality of an area and also refers to all the activities
285 that occur on the land surface (Wu et al., 2016). In the present study, LULC was classified into
286 six categories, namely, barren rocky land with occasional scrubs, cropland, fallow land, forest
287 and plantation, rural and urban settlements and water bodies, which covers an area of about 287
288 km^2, 611 km^2, 359 km^2, 407 km^2, 66 km^2, and 61 km^2 respectively. The LULC map is shown in
289 Fig. 2i.

290 The lineaments in the geological units are mainly the linear fractures detected on satellite images
291 and aerial photographs. Several researchers have advocated the positive relationship between
292 groundwater flow and yield with respect to the lineament density. Thus, detailed information on
293 the presence of lineaments in sub-surface lithological units are very important for groundwater
294 development and management studies (Al-Rawabdeh et al., 2015). The possibility of
295 groundwater pollution is increased due to the availability of higher lineament density that
296 promotes the infiltration of contaminants into groundwater. In the present study, lineament
297 density was classified into six subclasses i.e., 0-0.5 km/km^2, which encompasses over an area of
298 about 1391 km^2, 0.5-1 km/km^2, 1-1.5 km/km^2, 1.5-2.0 km/km^2, 2-2.5 km/km^2 and more than 2.5

299 km/km^2 extends over an area around 157 km^2, 61 km^2, 51 km^2, 33 km^2 and 91 km^2 respectively.
300 The prepared lineament density map is shown as Fig. 2j.

301 4. 2 Delineation of potential fluoride contaminated zones (FCZ)

302 As discussed earlier in section 3.2, factors weight and rating were assigned based on a
303 knowledge based AHP-based multi-criteria decision analysis (MCDM) and then potential
304 fluoride contaminated zones (FCZ) map was obtained by overlaying all the ten thematic layers in
305 Arc GIS 10.3 software. Figure 3(a) illustrates the distribution of potential fluoride contaminated
306 zones in the study area that implied the maximum and minimum indices values of the final
307 output within a range of 4.05 to 8.29. Thereafter, by using the "jenks natural breaks", the FCZ
308 map was classified into two categories namely, safe and unsafe zones with respect to fluoride
309 contamination. The safe zone means an area having fluoride concentration less than 1.5 mg/L,
310 whereas, the unsafe zone indicates the area with fluoride concentration higher than the
311 permissible limit, i.e., above 1.5 mg/L (BIS, 2012).
312 Based on the FCZ map (Fig. 3a), some parts of the study region belong to the safe category
313 covering an area of 1101.82 km^2 (61.52% of the total area). Groundwater from these zones is
314 suitable for drinking and other uses whereas, mostly the southeastern, southwestern parts and a
315 few stretches in the upper central northern portions were reflected as higher fluoride
316 contamination zones/ unsafe zones, covering an area of about 689.18 Km^2 (38.48% of the total
317 area) was unsuitable for drinking. Afterward, the reported unsafe zones were compared with the
318 geology of the area which indicates that these regions were underlain by granite-gneiss/granites
319 with intensely fractured basement rocks. The relatively higher ratings assigned to the existing
320 litho-units and structural features, including faults during the model computation process and are
321 forming the basis for assigning these areas as responsible as unsafe zones.

322 Furthermore, the results of the present study are in concurrence with the earlier studies
323 conducted by Kumar et al., (2017 and 2019) with the aid of hydro-geochemical signatures that
324 the elevated fluoride values are reported in the study area were of the geogenic source (granite
325 gneiss). Additionally, barren rocky land with occasional scrubs and the existence of cropland
326 may also contribute to elevated fluoride in groundwater being one of the prime anthropogenic
327 sources in a few places albeit to the lower extent. Similarly, the presence of pediplains and
328 relatively high rainfall distribution were also one of the leading factors responsible for the
329 contribution of high fluoride concentration which in turn results in an unsafe zone.

330 **"Figure 3 is about here"**

331 ## 4. 3 Validation of the proposed fluoride contamination zone (FCZ) map

332 In general, the AHP-based MCDM approach works with certain assumptions while assigning
333 ratings and weights purely based on the inputs provided by the modeler. Any error or imprecise
334 invoking of input parameters into the model may lead to erroneous results and thereby by the
335 failure of the approach. Therefore, it is imperative to validate the results obtained through the
336 knowledge based AHP-based MCDM approach model with the real ground conditions, in order
337 to avoid the uncertainties, if any. This will also ensure the accuracy and precision of the model.
338 For this sake, sixty-one groundwater samples covering the entire study area were collected
339 during May 2014 and analyzed for fluoride concentrations were overlaid on the final FCZ map.
340 Figure 3b shows the superimposition of on-site fluoride sampling locations with the prepared
341 fluoride contamination zone map. Thereafter, an agreement between predicted FCZ (pixel with
342 FCZ values) and the measured fluoride concentration of respective locations have been checked
343 (Table 3). Overall, 52 wells out of 61 wells with fluoride concentrations are having an agreement

concerning the respective fluoride contaminated zones. Therefore, it is prudent to conclude that the map of FCZ zones predicts the occurrence of fluoride contamination with 85.24% accuracy.

"Table 3 is about here"

5.0 Conclusions

In the present work, a knowledge based MCDM based model coupled with the application of remote sensing and GIS techniques has been proven to be an efficient tool for mapping fluoride contamination zones (FCZ) using selected hydro-geo-meteorological parameters. The findings were confirmed with a real fluoride concentration in wells obtained from 61 locations. The validation of actual fluoride concentration with the proposed model exhibited an agreement of around 85%, signifying the accuracy of the final model output. The results of the study revealed that 61.52% of the total area appeared as a safe zone, whereas 38.48 % of the total area emerged as unsafe zones i.e., areas with more than 1.5 mg/L fluoride concentration in groundwater.

The main advantage of the current study was the integration of a number of the hydro-geo-meteorological thematic layers on a regional scale that can be successfully adapted to delineate fluoride contaminated zones. In addition to this, the preciseness of model output to measure the authenticity and reliability level can also be taken into consideration by cross checking the generated output map with measured fluoride concentrations. Similarly, the major constraint of this approach is the absence of comprehensive information on a regional scale, especially for uneven distribution of reported fluoride point data and mineralogical composition of the rocks. In spite of this limitation, such type of FCZ mapping has been attempted first time in the study area in order to provide an insight into the potential fluoride contaminated zones. The FCZ map will

be very much helpful for the researchers, planners, and administrators in assessing the severity of contamination of fluoride concentration in groundwater. The FCZ map will also be helpful for evaluating the regions of the study area in the need of drinking water free from fluoride contamination. The unsafe zones can be identified for the construction of artificial recharge structures for diluting the concentration of fluoride in groundwater along with other remedial measures.

Acknowledgements

The authors express sincere thanks to the IIT (ISM), Dhanbad and CGWB management for the facilities extended towards the publication of this paper. The ideology addressed in this paper, solely belongs to the authors only and not necessarily of their organizations.

References

Adimalla, N., Marsetty, S.K. and Xu, P., 2019. Assessing groundwater quality and health risks of fluoride pollution in the Shasler Vagu (SV) watershed of Nalgonda, India. Human and Ecological Risk Assessment: An International Journal, pp.1-20.

Adimalla, N. and Venkatayogi, S., 2017. Mechanism of fluoride enrichment in groundwater of hard rock aquifers in Medak, Telangana State, South India. Environmental Earth Sciences, 76(1), p.45.

Al-Abadi, A.M., Al-Shamma'a, A.M. and Aljabbari, M.H., 2017. A GIS-based DRASTIC model for assessing intrinsic groundwater vulnerability in northeastern Missan governorate, southern Iraq. Applied Water Science, 7(1), pp.89-101.

Al-Rawabdeh, A.M., Al-Ansari, N.A., Al-Taani, A.A., Al-Khateeb, F.L. and Knutsson, S., 2014. Modeling the risk of groundwater contamination using modified DRASTIC and GIS in Amman-Zerqa Basin, Jordan. Central European Journal of Engineering, 4(3), pp.264-280.

Ando, M., Tadano, M., Yamamoto, S., Tamura, K., Asanuma, S., Watanabe, T., Kondo, T., Sakurai, S., Ji, R., Liang, C. and Chen, X., 2001. Health effects of fluoride pollution caused by coal burning. Science of the total environment, 271(1-3), pp.107-116.

Arulbalaji, P., Padmalal, D. and Sreelash, K., 2019. GIS and AHP techniques based delineation of groundwater potential zones: a case study from southern Western Ghats, India. Scientific reports, 9(1), pp.1-17.

Bagyaraj, M., Ramkumar, T., Venkatramanan, S. and Gurugnanam, B., 2013. Application of remote sensing and GIS analysis for identifying groundwater potential zone in parts of Kodaikanal Taluk, South India. Frontiers of Earth Science, 7(1), pp.65-75.

CGWB (Central Ground Water Board), 2013. Ground Water Information Booklet, Jamui District, Bihar, India. p.4.

Dartan, G.U.L.E.R., Taspinar, F.A.T.I.H. and Toroz, I., 2017. Analysis of fluoride pollution from fertilizer industry and phosphogypsum piles in agricultural area. J. Ind. Pollut. Control, 33, pp.662-669.

Elewa, H.H. and Qaddah, A.A., 2011. Groundwater potentiality mapping in the Sinai Peninsula, Egypt, using remote sensing and GIS-watershed-based modeling. Hydrogeology Journal, 19(3), pp.613-628.

GSI (Geological Survey of India), 1987. A Geoscientific appraisal of Munger district, Bihar for rural development, Bulletin series B No. 49, GSI, Government of India. Plate V.

Ghazavi, R. and Ebrahimi, Z., 2015. Assessing groundwater vulnerability to contamination in an arid environment using DRASTIC and GOD models. International journal of environmental science and technology, 12(9), pp.2909-2918.

Gonçalves, M.V.P., Santos, R.A., Coutinho, C.A.M. and Cruz, M.J.M., 2020. Fluoride Levels in the Groundwater and Prevalence of Dental Fluorosis in the Municipality of Santana, in Region Karstic of West Bahia, Brazil. In Groundwater Hydrology. Intech Open.DOI: http://dx.doi.org/10.5772/ intechopen.85007.

Ibrahim-Bathis, K. and Ahmed, S.A., 2016. Geospatial technology for delineating groundwater potential zones in Doddahalla watershed of Chitradurga district, India. The Egyptian Journal of Remote Sensing and Space Science, 19(2), pp.223-234.

Kim, K. and Jeong, G.Y., 2005. Factors influencing natural occurrence of fluoride-rich groundwaters: a case study in the southeastern part of the Korean Peninsula. Chemosphere, 58(10), pp.1399-1408.

Kumar, S., Singh, R., Venkatesh, A.S., Udayabhanu, G. and Sahoo, P.R., 2019. Medical Geological assessment of fluoride contaminated groundwater in parts of Indo-Gangetic Alluvial plains. Scientific reports, 9(1), pp.1-16.

Kumar, S., Venkatesh, A.S., Singh, R., Udayabhanu, G. and Saha, D., 2018. Geochemical signatures and isotopic systematics constraining dynamics of fluoride contamination in groundwater across Jamui district, Indo-Gangetic alluvial plains, India. Chemosphere, 205, pp.493-505. https://doi.org/10.1016/j.chemosphere.2018.04.116.

Liu G, Ye Q, Chen W, Zhao Z, Li L and Lin P. 2015. Study of the relationship between the lifestyle of residents residing in fluorosis endemic areas and adult skeletal fluorosis. Environ. Toxicol. Pharmacol. 40 (1), 326–332.

Luo, W., Gao, X. and Zhang, X., 2018. Geochemical processes controlling the groundwater chemistry and fluoride contamination in the Yuncheng Basin, China—An area with complex hydrogeochemical conditions. PloS one, 13(7).

Machiwal, D., Jha, M.K. and Mal, B.C., 2011. Assessment of groundwater potential in a semi-arid region of India using remote sensing, GIS and MCDM techniques. Water resources management, 25(5), pp.1359-1386.

Madhnure, P., Sirsikar, D.Y., Tiwari, A.N., Ranjan, B. and Malpe, D.B., 2007. Occurrence of fluoride in the groundwaters of Pandharkawada area, Yavatmal district, Maharashtra, India. Current Science, pp.675-679.

Mondal, N.C., Prasad, R.K., Saxena, V.K., Singh, Y. and Singh, V.S., 2009. Appraisal of highly fluoride zones in groundwater of Kurmapalli watershed, Nalgonda district, Andhra Pradesh (India). Environmental Earth Sciences, 59(1), pp.63-73.

Pillai, K.S. and Stanley, V.A., 2002. Implications of fluoride--an endless uncertainty. Journal of Environmental Biology, 23(1), pp.81-87.

Preeja, K. R., Joseph, S., Thomas, J., and Vijith, H., 2011. Identification of groundwater potential zones of a tropical river basin (Kerala, India) using remote sensing and GIS techniques. Journal of the Indian Society of Remote Sensing, 39(1), pp.83-94.

Rahman, M.M., Bodrud-Doza, M., Siddiqua, M.T., Zahid, A. and Islam, A.R.M.T., 2020. Spatiotemporal distribution of fluoride in drinking water and associated probabilistic human health risk appraisal in the coastal region, Bangladesh. Science of The Total Environment, 724, p.138316.

Rao, N.S., 2009. Fluoride in groundwater, Varaha River Basin, Visakhapatnam District, Andhra Pradesh, India. Environmental Monitoring and Assessment, 152(1-4), p.47.

Rashid, M., Lone, M.A. and Ahmed, S., 2012. Integrating geospatial and ground geophysical information as guidelines for groundwater potential zones in hard rock terrains of south India. Environmental monitoring and assessment, 184(8), pp.4829-4839.

Saaty, T.L., 1980. The analytic hierarchy process: planning, priority setting, resource allocation (McGraw-Hill International Book Company).

Saaty, T.L., 2004. Fundamentals of the analytic network process—multiple networks with benefits, costs, opportunities and risks. Journal of systems science and systems engineering, 13(3), pp.348-379.

Sawangjang, B., Hashimoto, T., Wongrueng, A., Wattanachira, S. and Takizawa, S., 2019. Assessment of fluoride intake from groundwater and intake reduction from delivering bottled water in Chiang Mai Province, Thailand. Heliyon, 5(9), p. e 02391.

Senthilkumar, P., Nithya, J. and Babu, S.S., 2014. Assessment of groundwater vulnerability in Krishnagiri District, Tamil Nadu, India using DRASTIC approach. International Journal of Innovative Research in Science, Engineering and Technology, 3(3), p-253.

Shanker, R., Thussu, J.L. and Prasad, J.M., 1987. Geothermal studies at Tattapani hot spring area, Sarguja district, central India. Geothermics, 16(1), pp.61-76.

Singh, R., Syed, T.H., Kumar, S., Kumar, M. and Venkatesh, A.S., 2017b. Hydrogeochemical assessment of surface and groundwater resources of Korba coalfield, Central India: environmental implications. Arabian Journal of Geosciences, 10(14), p.318.

Singh, R., Venkatesh, A.S., Syed, T.H., Reddy, A.G.S., Kumar, M. and Kurakalva, R.M., 2017a. Assessment of potentially toxic trace elements contamination in groundwater resources of the coal mining area of the Korba Coalfield, Central India. Environmental Earth Sciences, 76(16), p.566.

Singh, R., Venkatesh, A.S., Syed, T.H., Surinaidu, L., Pasupuleti, S., Rai, S.P. and Kumar, M., 2018. Stable isotope systematics and geochemical signatures constraining groundwater hydraulics in the mining environment of the Korba Coalfield, Central India. Environmental Earth Sciences, 77(15), p.548.

Singha, S.S., Pasupuleti, S., Singha, S., Singh, R. and Venkatesh, A.S., 2019a. Analytic network process based approach for delineation of groundwater potential zones in Korba district, Central India using remote sensing and GIS. Geocarto International, pp.1-23.

Singha, S., Pasupuleti, S., Durbha, K.S., Singha, S.S., Singh, R. and Venkatesh, A.S., 2019b. An analytical hierarchy process-based geospatial modeling for delineation of potential anthropogenic contamination zones of groundwater from Arang block of Raipur district, Chhattisgarh, Central India. Environmental Earth Sciences, 78(24), p.694.

Singha, S., Pasupuleti, S. and Villuri, V.G.K., 2017. An integrated approach for evaluation of groundwater quality in Korba district, Chhattisgarh using Geomatic techniques. Journal of Environmental Biology, 38(5), p.865.

Srivastava, S.K. and Ramanathan, A.L., 2018. Geochemical assessment of fluoride enrichment and nitrate contamination in groundwater in hard-rock aquifer by using graphical and statistical methods. Journal of Earth System Science, 127(7), p.104.

Su, H., Wang, J. and Liu, J., 2019. Geochemical factors controlling the occurrence of high-fluoride groundwater in the western region of the Ordos basin, northwestern China. Environmental pollution, 252, pp.1154-1162.

Thapa, R., Gupta, S. and Kaur, H., 2017. Delineation of potential fluoride contamination zones in Birbhum, West Bengal, India, using remote sensing and GIS techniques. Arabian Journal of Geosciences, 10(23), p.527.

Thapa, R., Gupta, S., Guin, S. and Kaur, H., 2018. Sensitivity analysis and mapping the potential groundwater vulnerability zones in Birbhum district, India: A comparative approach between vulnerability models. Water Science, 32(1), pp.44-66.

Todd, K. D. and Mays. L.W., 2005. Groundwater Hydrology. Third ed. John Wiley and Sons, p.636.

Tossou, Y.Y.J., Orban, P., Gesels, J., Otten, J., Yessoufou, S., Boukari, M. and Brouyère, S., 2017. Hydrogeochemical mechanisms governing the mineralization and elevated fluoride $$\left ({\text {F}^{-}}\right) $$ contents in Precambrian crystalline aquifer groundwater in central Benin, Western Africa. Environmental Earth Sciences, 76(20), p.691.

Vithanage, M., Rajapaksha, A.U., Bootharaju, M.S. and Pradeep, T., 2014. Surface complexation of fluoride at the activated nano-gibbsite water interface. Colloids and Surfaces A: Physicochemical and Engineering Aspects, 462, pp.124-130.

Wu, H., Chen, J. and Qian, H., 2016. A modified DRASTIC model for assessing contamination risk of groundwater in the northern suburb of Yinchuan, China. Environmental Earth Sciences, 75(6), p.483.

Xu, Y., Huang, H., Zeng, Q., Yu, C., Yao, M., Hong, F., Luo, P., Pan, X. and Zhang, A., 2017. The effect of elemental content on the risk of dental fluorosis and the exposure of the environment and population to fluoride produced by coal-burning. Environmental Toxicology and Pharmacology, 56, pp.329-339.

591 **List of Tables**

592 **Table 1:** Details of the ten thematic layers along with their areal extents.

Parameter	Subclass	Rating	Normalized weight	Area (km^2)	Percentage area (%)
Aquifer	Alluvial	4	0.195	113.67	6.35
	Biotite-muscovite-chloride schist	8		818.47	45.70
	Granite gneiss	10		505.75	28.24
	Quartizite, quartz schist and phyllite	5		353.11	19.72
Geomorphology	Alluvial plain	4	0.096	463.2	25.86
	Denundational hill and Piedmont	3		729.7	40.74
	Pediplain	9		598.1	33.39
Soil texture	Coarse loamy soil	9	0.166	457.60	25.55
	Fine loamy soil	5		1333.40	74.45
Slope (%)	0-3%	9	0.021	653.67	36.50
	3-6%	7		625.73	34.94
	6-9%	5		210.02	11.73
	9-12%	3		64.59	3.61
	>12%	1		236.99	13.23
Elevation	42-167	9	0.021	1414.77	78.99
	167-292	6		297.35	16.60
	292-417	3		69.71	3.89
	417-542	1		9.17	0.51
Drainage density (km/km^2)	0-3	9	0.100	1264.49	70.60
	3 to 6	7		369.23	20.62
	6 to 9	5		103.7	5.79
	9 to 12	2		44.71	2.50
	>12	1		8.87	0.50
Rainfall (mm/year)	718-835	4	0.120	116.85	6.52
	835-952	6		1224.71	68.38
	>952	8		449.44	25.09
Depth to water table (m)	0 to 3	3	0.170	4.63	0.26
	3 to 6	5		1137.98	63.54
	6 to 9	7		633.77	35.39
	> 9	9		14.62	0.82
Land use land cover	Barren rocky land with occasional scrub	9	0.077	287.39	16.05
	Crop land	7		611.32	34.13
	Fallow land	3		358.83	20.04
	Forrest and plantation	4		406.72	22.71
	Rural and urban settlement	1		65.82	3.68
	Water body	2		60.92	3.40
Lineament density (km/km^2)	0-0.5	2	0.034	1390.87	77.66
	0.5-1.0	3		156.77	8.75
	1.0-1.5	4		60.82	3.40
	1.5-2.0	5		50.81	2.84

	2.0-2.5	6	33.12	1.85
	>2.5	7	98.61	5.51

593

594

595 **Table 2:** Pair wise comparison matrix established amidst ten thematic layers.

Parameter	P1	P2	P3	P4	P5	P6	P7	P8	P9	P10
P1	1.00	2.00	1.00	3.00	3.00	2.00	2.00	4.00	6.00	6.00
P2	0.50	1.00	1.00	3.00	3.00	2.00	3.00	3.00	5.00	5.00
P3	1.00	1.00	1.00	2.00	2.00	2.00	3.00	4.00	6.00	6.00
P4	0.33	0.33	0.50	1.00	2.00	2.00	3.00	4.00	5.00	5.00
P5	0.33	0.33	0.50	0.50	1.00	1.00	3.00	4.00	6.00	6.00
P6	0.50	0.50	0.50	0.50	1.00	1.00	2.00	3.00	6.00	6.00
P7	0.50	0.33	0.33	0.33	0.33	0.50	1.00	5.00	6.00	6.00
P8	0.25	0.33	0.25	0.25	0.25	0.33	0.20	1.00	2.00	2.00
P9	0.17	0.20	0.17	0.20	0.17	0.17	0.17	0.50	1.00	1.00
P10	0.17	0.20	0.17	0.20	0.17	0.17	0.17	0.50	1.00	1.00

596

597

598 **Table 3.**Agreement details of measured fluoride concentration with fluoride contamination zones.

Sr	Location	Longitude	Latitude	Type of Sample	Catchment Area (Lithology)	Fluoride concentration (mg/L)	Zone	Agreement
1	Bhimbandh	86.3750	25.0620	HP		0.01	6.09	Agree
2	Sikandara	86.0500	24.9333	HP	Alluviam	0.08	6.71	Disagree
3	Maniadda	86.2109	24.9580	HP	Alluviam	0.14	6.43	Agree
4	Nawadi	86.0000	24.9020	HP	Alluviam	0.14	6.57	Agree
5	Corporation Bank	86.1569	24.9267	HP	Alluviam	0.18	6.47	Agree
6	Kala	86.4085	24.9654	HP	Hard rock	0.20	6.06	Agree
7	Manjhos	86.1043	24.9600	HP	Alluviam	0.21	5.72	Agree
8	Bhemain	86.2176	24.7882	HP	Alluviam	0.22	6.16	Agree
9	Domachak	86.4108	24.9980	HP	Hard rock	0.23	6.70	Disagree
10	Amaratah	86.1883	24.9536	HP	Alluviam	0.26	5.90	Agree
11	lakshmipur	86.4031	25.0069	HP	Hard rock	0.26	6.30	Agree
12	Ratanpur	86.2868	24.8992	HP	Alluviam	0.36	6.00	Agree
13	Jogia	86.4032	25.0249	HP		0.38	5.65	Agree
14	Fatehpur	86.1879	24.8085	HP	Hard rock	0.44	6.35	Agree
15	Kamat	86.2525	24.7503	DW	Alluviam	0.51	5.62	Agree
16	Dighi	86.4309	24.9356	HP	Alluviam	0.52	6.03	Agree
17	jhajha	86.3628	24.7890	HP	Hard rock	0.53	6.03	Agree
18	Purnakhaira	86.1921	24.8768	HP	Alluviam	0.53	6.43	Agree
19	Gidhour	86.3064	24.8564	HP	Hard rock	0.54	5.67	Agree
20	Sonai	86.1900	24.9954	HP	Alluviam	0.55	6.46	Agree
21	Guguldih	86.3181	24.9150	HP	Alluviam	0.61	6.22	Agree
22	Jhajah	86.3640	24.7890	DW	Hard rock	0.66	6.03	Agree
23	Middle School, Barahat	86.2939	25.0200	HP	Hard rock	0.67	5.78	Agree
24	Nawadi	86.0000	24.9000	DW	Alluviam	0.68	6.39	Agree
25	Lakhuar	86.0375	24.9611	DTW	Alluviam	0.70	5.88	Agree
26	Patneshwar Temple	86.2407	24.9637	HP	Hard rock	0.78	6.14	Agree
27	Dighoi	86.2139	24.9794	HP		0.83	6.52	Agree
28	Dehuridih	86.3000	24.7600	HP	Alluviam	0.88	4.98	Agree

29	JNV,Jamui	86.2950	25.0024	DTW	Hard rock	0.88	6.88	Disagree
30	Barakhua,Barahat	86.2804	24.9919	HP	Hard rock	0.91	6.50	Agree
31	Mahadeosimaria	86.1341	24.9168	DW	Alluviam	1.03	6.71	Disagree
32	Mangobandar	86.2656	24.8153	HP	Hard rock	1.06	6.06	Agree
33	Hardimoh	86.2582	24.8464	HP	Hard rock	1.08	6.22	Agree
34	Cinbaria	86.3410	24.9432	HP	Alluviam	1.17	6.27	Agree
35	Magahi	86.3821	24.8845	HP	Hard rock	1.18	6.91	Disagree
36	Kenuhat	86.3723	24.9908	HP	Hard rock	1.27	5.91	Agree
37	Sandipi	86.4128	24.9354	HP	Hard rock	1.32	6.38	Agree
38	Dhamna	86.3578	24.8521	HP	Hard rock	1.39	5.52	Agree
39	Gidheswar	86.1799	24.8155	DW	Hard rock	1.40	6.62	Agree
40	ItaSagar	86.0915	24.9108	HP	Hard rock	1.55	6.00	Disagree
41	Numer	86.2967	24.9667	HP	Hard rock	1.56	6.81	Agree
42	Sindhu Mahodar	86.4794	24.9071	HP		1.57	7.13	Agree
43	Bhelbindo	86.4458	24.8270	HP	Hard rock	1.63	7.41	Agree
44	Ragatraunia	86.3705	24.7414	HP		1.63	7.83	Agree
45	Darima	86.1297	24.7954	HP		1.70	6.75	Agree
46	New AbadiGanj	86.3844	24.7865	HP	Hard rock	1.72	7.72	Agree
47	Sarebad	86.2073	24.7671	DW	Alluviam	1.89	7.10	Agree
48	Harna	86.4100	24.7593	DW	Hard rock	2.10	8.09	Agree
49	Bishanpur	86.3160	24.9840	TW	Hard rock	2.21	7.20	Agree
50	Nargango	86.3544	24.7454	HP		2.40	7.68	Agree
51	Jokatia	86.3544	24.7454	HP		2.70	7.68	Agree
52	Lalmatia	86.3000	24.9829	HP	Hard rock	2.90	7.66	Agree
53	Chandresekhar Nagar	86.3553	24.8916	HP	Hard rock	3.00	7.24	Agree
54	Primary S chooljeevanTola	86.3800	24.8000	HP	Hard rock	3.08	7.37	Agree
55	Bhadwaria	86.4624	24.7635	HP		3.25	6.72	Agree
56	Majhwe	86.1464	25.0360	HP	Hard rock	3.30	6.79	Agree
57	Prakash Nagar	86.3880	24.8141	HP	Hard rock	3.34	6.51	Disagree
58	Panch Pahari	86.3362	24.7469	HP		3.50	7.63	Agree
59	Nabinagar	86.1572	25.0292	DTW	Hard rock	5.30	6.78	Agree
60	Malaypur	86.2625	24.9717	DTW	Hard rock	5.60	6.35	Disagree
61	Majhwe	86.2625	24.9717	DTW	Hard rock	5.80	6.35	Disagree

610

611 **List of Figures**

612 **Figure 1:** Methodology adopted for portraying fluoride contamination zones (FCZ) in the
613 research area.

614 **Figure 2:** Spatial distribution of different thematic layers (a) Aquifer map (b) Geomorphological
615 pattern (c) Soil texture map (d) Slope map (e) Elevation map (f) Drainage density (g) Rainfall
616 distribution (h) Depth to water table (i) Land use land cover pattern (j) Lineament density map of
617 the study area.

618 **Figure 3**. (a) Fluoride contamination zone (FCZ) map of the study area. (b) Superimposition of
619 observation wells on the FCZ map.

620

621

622

Figures

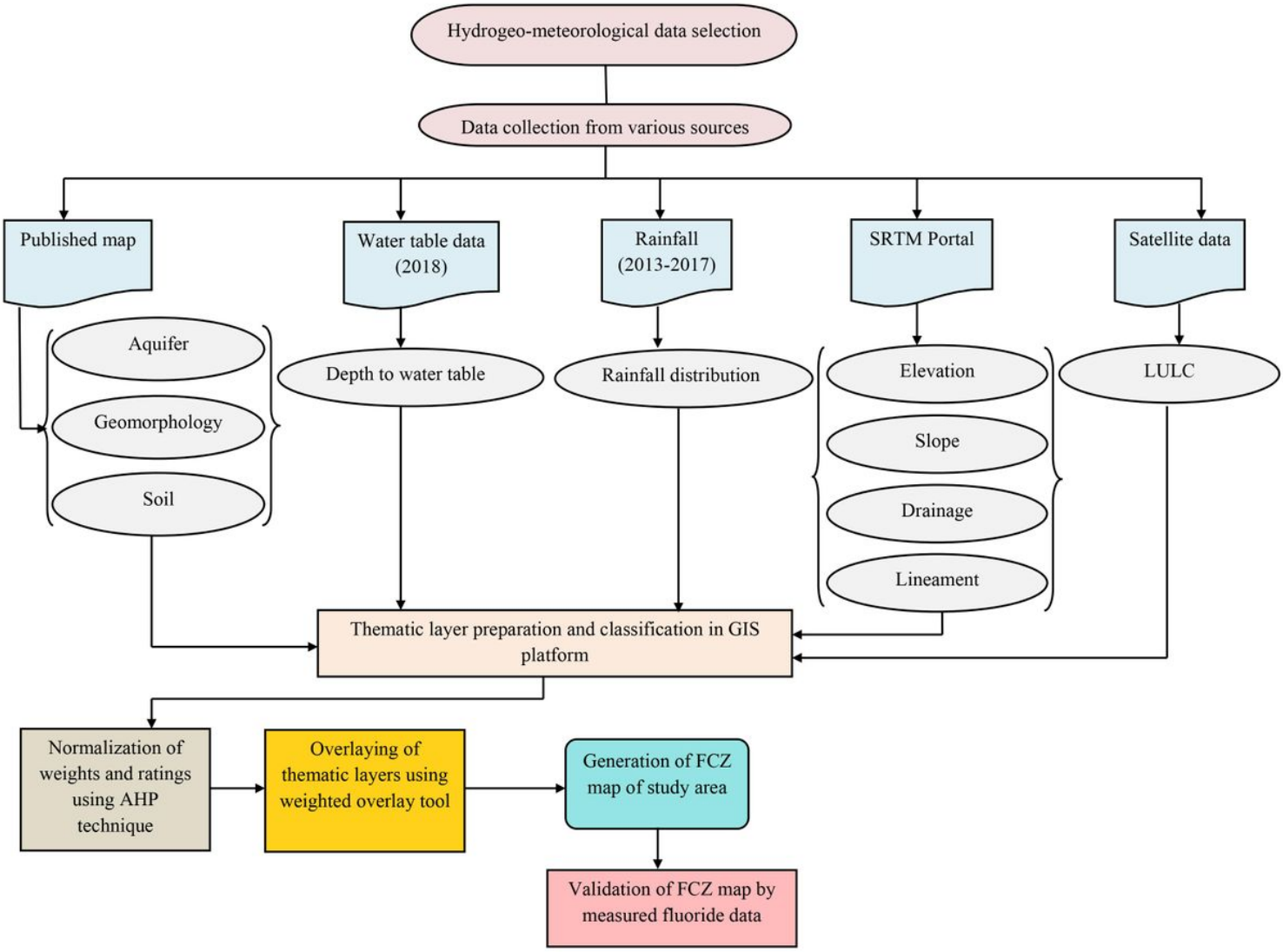

Figure 1

Methodology adopted for portraying fluoride contamination zones (FCZ) in the research area.

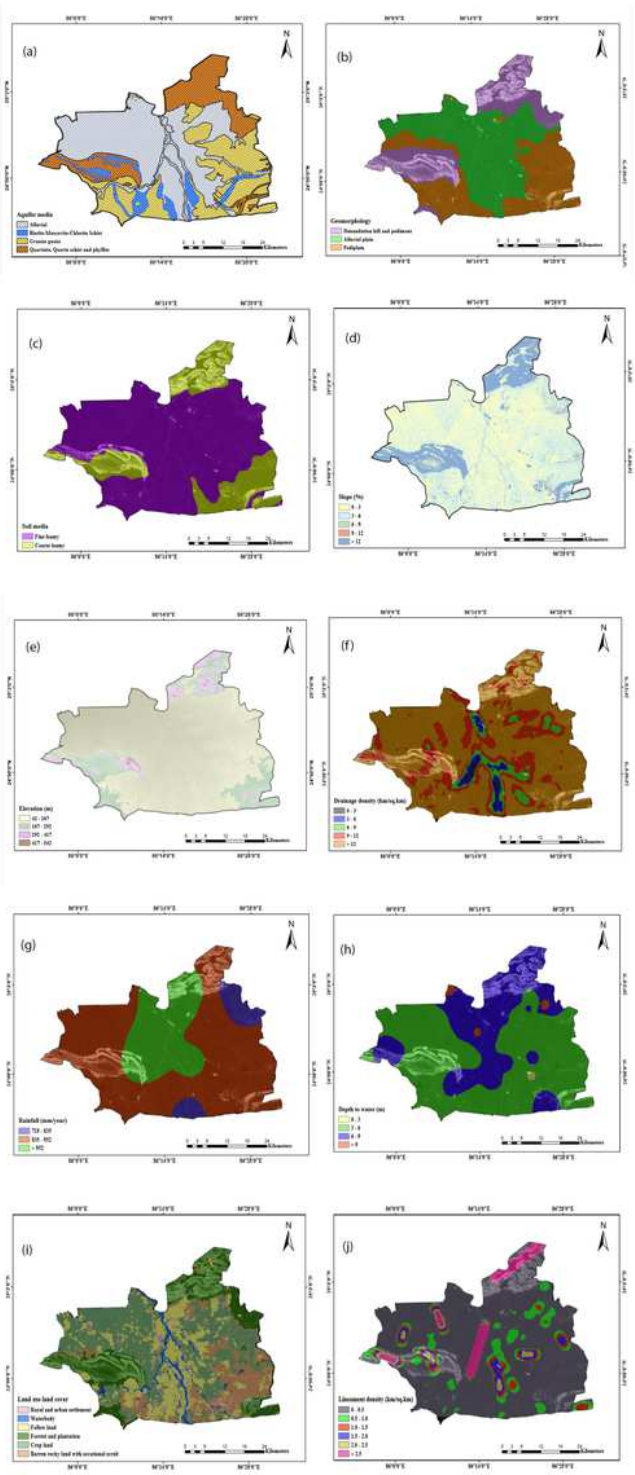

Figure 2

Spatial distribution of different thematic layers (a) Aquifer map (b) Geomorphological pattern (c) Soil texture map (d) Slope map (e) Elevation map (f) Drainage density (g) Rainfall distribution (h) Depth to water table (i) Land use land cover pattern (j) Lineament density map of the study area. Note: The designations employed and the presentation of the material on this map do not imply the expression of any opinion whatsoever on the part of Research Square concerning the legal status of any country,

territory, city or area or of its authorities, or concerning the delimitation of its frontiers or boundaries. This map has been provided by the authors.

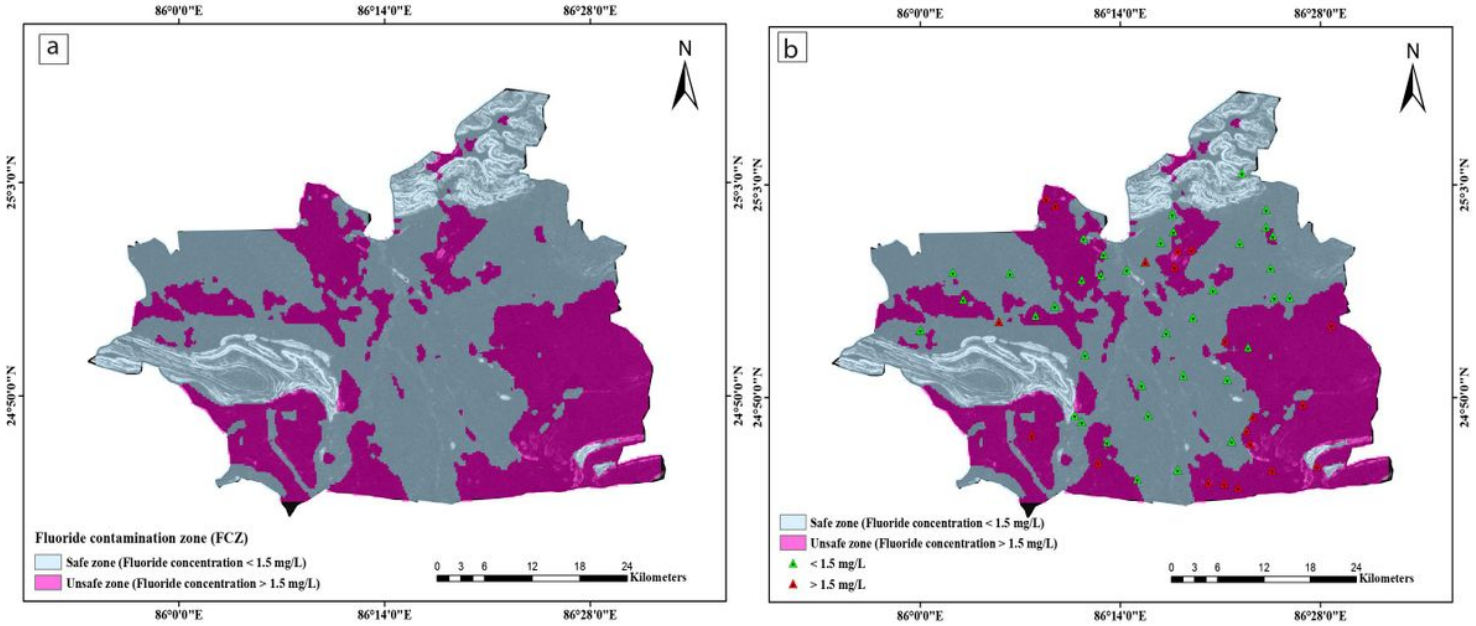

Figure 3

(a) Fluoride contamination zone (FCZ) map of the study area. (b) Superimposition of observation wells on the FCZ map. Note: The designations employed and the presentation of the material on this map do not imply the expression of any opinion whatsoever on the part of Research Square concerning the legal status of any country, territory, city or area or of its authorities, or concerning the delimitation of its frontiers or boundaries. This map has been provided by the authors.